RSC Advances

PAPER

View Article Online
View Journal | View Issue

Cite this: *RSC Adv.*, 2025, **15**, 32721

Optimizing dual hierarchical textured superhydrophobic paper for enhanced writing and printing performance: balancing water resistance and ink adhesion

V. G. C. Samanmali,[ad] A. R. M. A. M. Rathnayake,[ad] Nishan Dharmaweera,[b] T. Bandara,[c] R. T. De Silva[d] and M. M. M. G. P. G. Mantilaka *[d]

Superhydrophobic printable and writable cellulose paper preparation requirements are becoming increasingly significant in the current climate for a variety of important applications. The present work introduces a simple and successful approach for creating a superhydrophobic paper that can be printed and written on while maintaining its water repellent properties. The paper is coated with modified silica utilizing tetraethyl orthosilicate (TEOS), methyltriethoxysilane (MTES), 1H, 1H, 2H, 2H – perfluorooctyltriethoxysilane (PFOTES), and acrylic binder *via* a dip coating process. As a result of multi-layer deposition of silicon dioxide (SiO_2) microbeads with nano-micro size mountain-like wrinkled coating on each bead, the treated paper develops a nano/microstructure with a water contact angle (WCA) of 152° ± 2° and a water sliding angle (WSA) of 7° ± 0.5°. This superhydrophobic surface retains its superhydrophobicity after 50 abrasion cycles on sandpaper and maintains its self-cleaning property with soil particles and many types of liquids. The superhydrophobic paper products have a higher tensile strength (~6 MPa) than non-treated paper (~2 MPa) while preserving superhydrophobicity across pH ranges 5–11. The treated papers show excellent printability and writability and retain their superhydrophobicity after printing and writing. This superhydrophobic paper can be used to create waterproof paper-based printed products and artwork.

Received 12th August 2025
Accepted 27th August 2025

DOI: 10.1039/d5ra05937b

rsc.li/rsc-advances

1 Introduction

Currently, superhydrophobic surfaces and coatings are a widely discussed topic due to their remarkable applications, such as anti-corrosion,[1,2] oil-water separation,[2,3] anti-icing,[4,5] anti-fogging,[6,7] and self-cleaning.[5,8] A superhydrophobic surface is a surface that has a water contact angle (WCA) more than 150° and a water sliding angle (WSA) less than 10°. This means that when a water droplet lands on the superhydrophobic surface, it forms almost a perfect sphere and can easily roll off from the surface.[9,10] Superhydrophobic surfaces require a combination of low surface energy and substantial surface roughness.[11,12] When a water droplet sits on a rough surface, it comes into contact with both the materials that make up the surface and the air pockets within the structure. Since air inherently exhibits a contact angle of 180°, indicating its hydrophobic nature, the introduction of surface roughness further enhances the superhydrophobic properties of the surface.[9,13]

Water infiltration through the surface of cellulose-based papers causes deformation of the entire material, which is frequently employed in packaging, information recording, decoration, filtration, microfluidic device production, and currency.[14,15] Due to this crucial issue, the paper industry is focusing on developing superhydrophobic coatings to enhance the durability and resilience of papers.[14,15] Cellulose paper has high hydroxyl group content, making it hydrophilic and disintegrate in water.[15,16] Different industries, such as steel, glass, wood, plastic, and textiles, use a variety of surface-engineering techniques like chemical etching,[17,18] plasma treatment,[15,19] photolithography,[15,20] and nanoparticulate deposition[21,22] to create water-repellent surfaces. Cellulose can be readily degraded by wet-chemical or thermal treatments, hence the abovementioned techniques are inapplicable to cellulose-based papers.[15,23]

To form a waterproof surface on cellulosic papers, some techniques have been used, such as multilayer deposition of polydiallyldimethylammonium chloride and silicon dioxide (SiO_2) particles, followed by a fluorination surface treatment

[a]*Faculty of Graduate Studies, University of Sri Jayewardenepura, Gangodawila, Nugegoda, Sri Lanka*
[b]*Faculty of Engineering, University of Sri Jayewardenepura, 41 Lumbini Ave, Dehiwala Mount Lavinia, Sri Lanka*
[c]*Federation University Gippsland Campus, PO Box 3191, Glippsland Mail Center, Victoria 3841, Australia*
[d]*CodeGen International (Pvt) Ltd, Bay 1-5, Trace Expert City, Colombo 10, Sri Lanka. E-mail: mantilaka.publications@gmail.com*

with 1H,1H,2H,2H-perfluorooctyltriethoxysilane (PFOTES), coating of fluoro-containing SiO_2 nanoparticles prepared by cohydrolysis of tetraethyl orthosilicate (TEOS)/fluorinated alkyl silane with ammonia, and coating of organic nanoparticles.[9,24] Although various superhydrophobic methods have been developed for cellulose-based papers, most are impractically complex, lack enduring stability, and fail to retain their functionality under realistic use cases, particularly those involving writing and printing processes.[9,15]

In superhydrophobic coatings, perfluorinated compounds (*e.g.*, PFOTES) have been widely employed due to their exceptional ability to lower surface energy and repel water and oils effectively.[24] However, their use raises serious environmental and health concerns because of their persistence in ecosystems, bioaccumulative nature, and potential toxicity, including links to endocrine disruption and cancer.[25,26] These concerns have prompted a critical reassessment of material choices in superhydrophobic surface design. As a result, there is a growing shift in research toward developing fluorine-free alternatives (*e.g.*, methyltriethoxysilane (MTES), polydimethylsiloxane (PDMS)) that maintain high water repellency without compromising environmental safety.[27–29] Strategies include using bio-based materials (*e.g.*, beeswax, carnauba wax), silica nanoparticles with low-surface-energy polymers, or physical surface structuring (*e.g.*, micro/nano-texturing) that achieves superhydrophobicity through topography rather than chemical treatment.[26,30]

Considering the challenges associated with existing superhydrophobic paper coatings, this study aims to develop a novel superhydrophobic coating for cellulose-based papers that retains its surface properties even after writing and printing. This is a simple dip coating method with a one-day aging time to produce a long-lasting, highly resilient paper. This innovative approach utilizes a combination of TEOS with both fluorinated and fluorine-free silanes, aiming to enhance the hydrophobicity of the paper while reducing the environmental impact typically associated with fluorinated compounds.

2 Experimental

2.1 Materials

Tetraethyl orthosilicate (TEOS) with 98% purity (SiO_2 content 28–28.8%) was purchased from Access Labtech (Pvt) Ltd (Sri Lanka). Xylene (99%), acetic acid (99.9%), cellulose papers, and acrylic binder (Nippon acrylic clear coating [AC], spreading capacity – 75–85 square feet per litre) were obtained from the local market (Sri Lanka). The AC comprises a solid content of 15–32 wt% acrylic polymer and approximately 1 wt% amorphous SiO_2, uniformly dispersed in xylene. Here, the acrylic polymer is synthesized through the copolymerization of butyl acrylate, methacrylic acid, methyl methacrylate, and styrene. 1H, 1H, 2H, 2H – perfluorooctyltriethoxysilane (PFOTES) with 97% purity was received from Shandong Zhishang New Material Co., Ltd, China. Methyltriethoxysilane (MTES) with ≤100% purity was provided by Shanghai Starsky New Material Co., Ltd, China. All chemicals were used as received.

2.2 Sample preparation

Modified silica colloidal deposition serves as the foundation for this superhydrophobic paper product. Initially, 5 mL of TEOS was mixed with 50 mL of xylene (1 : 10) in a beaker at 500 rpm for 10 minutes. Next, 2.5 mL of MTES and PFOTES were added (1 : 1) and the mixture was agitated for another 10 minutes before adding acetic acid to raise the pH level to 3. Cellulose papers (5 cm × 5 cm) were immersed in the mixture after increasing the temperature to 80 °C and stirred at 150 rpm for 1 hour. After that, 5 mL of AC was added dropwise to the mixture and stirred for another 10 minutes.

The mixture, containing the cellulose papers, was then aged at room temperature for 24 hours, allowing the modified SiO_2 to settle uniformly across the surfaces. After 24 hours, dipped papers were removed from the solution and dried at 80 °C for an hour. The superhydrophobic papers were then tested and characterized using different techniques.

2.3 Characterization

The surface morphology of modified and unmodified papers was obtained using Hitachi SU6600 FE-SEM Scanning Electron Microscope (SEM) and the elemental distribution of treated paper was examined using the Energy-Dispersive X-ray (EDX) mapping images obtained from the SEM. The chemical analysis of paper samples was performed using Bruker Vertex80 Fourier Transform Infrared Spectrometer (FTIR). The hydrophobicity of papers was assessed by WCA measurements using Kruss (DSA25S) Drop Shape Analyzer, WSA measurements using ImageJ Software, and the surface asperity of engineered papers was examined using Park Systems XE 100 Atomic Force Microscope (AFM). All characterizations were carried out at the Sri Lanka Institute of Nanotechnology (SLINTEC) in Homagama, Sri Lanka.

2.4 Tests for self-cleaning and durability

Soil particles and mud were employed to test the self-cleaning ability of the modified paper. A layer of soil particles and a drop of mud were spread on the two treated papers, and water droplets were allowed to roll off from the surface of the contaminated superhydrophobic papers. The durability of the engineered paper was assessed by measuring the static WCA of water droplets on its surface, following exposure to various external disturbances. The superhydrophobic papers were subjected to a variety of external perturbations, including strong acid, strong base, and various everyday beverages such as tea, milk, coffee, carbonated beverages, malted beverages, and food dye. For acid–base chemical resistance testing, rectangular coated paper specimens (2 cm × 4 cm) were immersed in 20 mL of aqueous solutions with controlled pH values of 1, 3, 7, 11, and 13 for a duration of 1 hour at room temperature (~27 °C). Following immersion, the samples were thoroughly rinsed with deionized water to remove residual chemicals and were subsequently dried under ambient conditions. To evaluate any alterations in surface wettability resulting from chemical exposure, the static WCA was measured using deionized water

at neutral pH. This approach ensured consistent and reliable comparison of hydrophobic performance across all treated samples, independent of the pH of the immersion medium. Evaluation of the superhydrophobicity of the paper against mechanical abrasion was tested using a handcrafted abrasion testing apparatus.

2.5 Tests for mechanical strength

The tensile strength of both coated and uncoated papers was determined using an Instron 3365 Tensile Tester at the Sri Lankan Institute of Nanotechnology (SLINTEC) in Homagama, Sri Lanka. The average values at maximum stress were determined by measuring 4 samples of both coated and uncoated paper. The measurement was done using the paper's dimensions of 8 cm × 1 cm. To evaluate the mechanical flexibility of the superhydrophobic coating the treated paper was manually bent back and forth along the same axis several times to form a crease. In each bending, the crease was examined for any visible cracking, delamination, or loss of superhydrophobicity, such as reduced water repellency or localized wetting along the fold.

2.6 Tests for writability and printability

The writability and printability of the treated paper were evaluated to determine its suitability for practical applications. Writability was tested using a ballpoint pen, graphite pencil, and permanent marker to observe how different writing tools interact with the low surface energy surface. Printability was assessed using an inkjet printer (EPSON L130 Ink Tank Printer) and a laser printer (Toshiba E-Studio 3015AC Colour Laser Photocopier), representing both ink-based and toner-based printing technologies.

3. Results and discussion

3.1 Process of preparation of superhydrophobic cellulose paper *via* modified silica colloidal deposition

The fabrication of the superhydrophobic coating on cellulose paper is based on a sol–gel reaction mechanism involving the acid-catalyzed hydrolysis and condensation of organosilane precursors. In this process, TEOS was first dispersed in xylene, a nonpolar solvent chosen not only for its compatibility with the hydrophobic silanes and inert interaction with cellulose fibers but also for its ability to facilitate the formation of a homogeneous sol.[31] MTES and PFOTES were subsequently added to the precursor solution. Under acidic conditions (adjusted to pH ~3 using acetic acid), silanes undergo hydrolysis, producing reactive silanol (Si–OH) groups. These silanols then condensed to form siloxane (Si–O–Si) linkages, leading to the formation of a crosslinked silica network. MTES contributed methyl functionalities that lower surface polarity, while PFOTES introduced long-chain perfluoroalkyl groups that significantly reduce surface energy.[32,33] MTES was specifically selected as an alternative to significantly reduce the overall use of PFOTES, thereby lowering the fluorine content in the coating while preserving the desired superhydrophobic properties. As a result, the evolving silica sol becomes both structurally robust and chemically modified for surface functionalization.

Upon immersing cellulose paper into this reactive sol at elevated temperatures, the functionalized silica nanoparticles get adhered to the hydroxyl-rich cellulose fibers *via* hydrogen bonding and potential covalent bonding through siloxane linkages.[34,35] To further enhance the interfacial adhesion and mechanical durability of the coating, an adhesive component (Nippon AC) was incorporated directly into the same sol–gel bath. This acrylic-based binder consists of solid acrylic polymer and amorphous SiO_2, both dissolved in xylene, ensuring excellent miscibility with the sol–gel matrix. Here, this solid acrylic polymer was synthesized *via* the copolymerization of four types of monomers, resulting in a solvent-based film-forming binder that contributes structural reinforcement without compromising the surface energy profile of the coating. Its integration into the silica sol provides strong interfacial bonding between the inorganic silica phase and the organic cellulose substrate, thereby improving the coating's resistance to mechanical stress and environmental degradation.

Then the system was aged under ambient conditions to allow for complete gelation and network consolidation, driven by the continued condensation of residual silanol groups.[36] Volatile byproducts were eliminated through the final thermal treatment, which resulted in a permanently stabilized nanostructured, low-surface-energy layer and yielded a robust and durable superhydrophobic surface on the cellulose paper. The key innovation of this method was demonstrated through its single-step dip-coating approach, in which surface functionalization, structural reinforcement, and coating deposition were simultaneously achieved within one unified process. This contrasted with conventional multi-step protocols, where sol–gel synthesis, surface modification, and binder application are typically conducted separately, often requiring intermediate drying, curing, or chemical treatments.[15,24] By enabling the integration of sol–gel chemistry with polymeric adhesion in a single formulation, the proposed approach was established as a streamlined and scalable alternative for producing high-performance superhydrophobic coatings on cellulose papers. Process complexity and time were reduced, while interfacial incompatibilities were minimized, leading to improved coating uniformity and reproducibility.

3.2 Surface morphology and roughness

SEM image analysis was used to compare the surface texture of paper before and after superhydrophobic coating treatment. Cellulose papers are manufactured by connecting a large number of pure cellulose fibres as a network, providing a smooth surface (Fig. 1a and b).[12,37] After the superhydrophobic treatment, the smooth paper surface became rough due to the deposition of SiO_2 microbeads with nano-micro scale mountain-like wrinkled coating on each bead (Fig. 1c, d, e, and f). This micro-nano hierarchical structure of the treated paper surface increases the area of air trapping through multilayer deposition roughness of the coating, significantly enhancing hydrophobicity by reducing surface energy.[13,38,39] The SEM

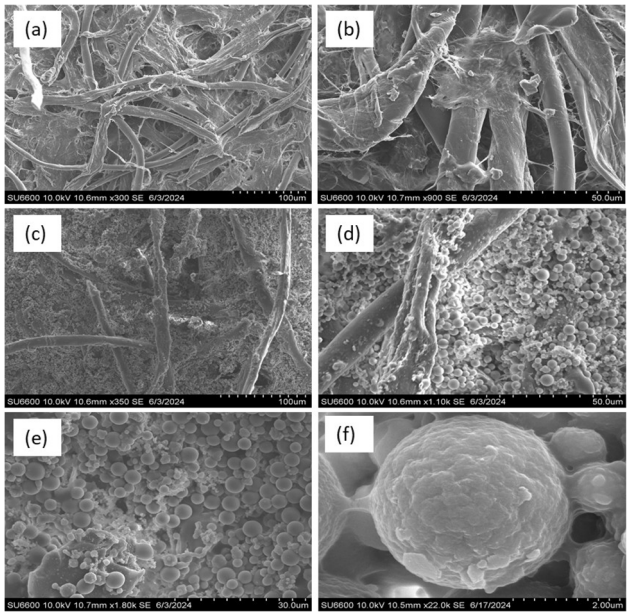

Fig. 1 SEM images of untreated papers (a) at low (b) at high magnification, treated paper with superhydrophobic coating (c) at low (d) at high magnification same magnification as the untreated paper images, (e) SiO_2 microbeads, and (f) SiO_2 microbeads covered by nano-micro scale mountain-like wrinkled structure.

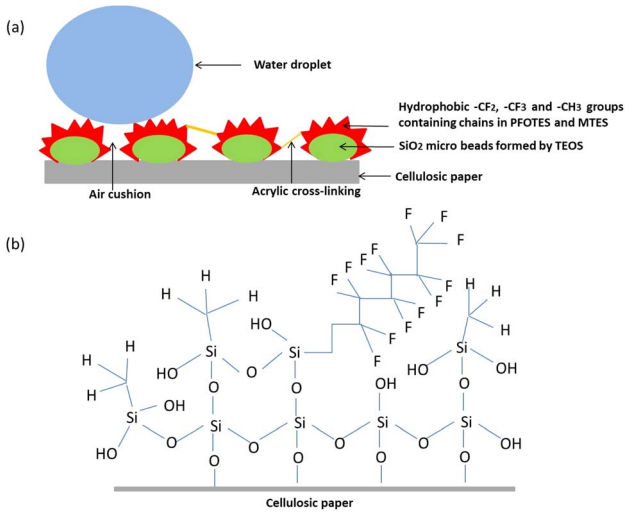

Fig. 2 (a) Schematic representation of the formation of the superhydrophobic layer on the paper surface, illustrating the processes of SiO_2 microbeads synthesis and silane modification combined with acrylic cross-linking, and (b) chemical structure showing the combination of TEOS, PFOTES, and MTES on the paper surface, highlighting the bonding interactions and formation of the hydrophobic layer.

images also revealed that the cross-linking of the acrylic binder between SiO_2 microbeads further enhances the hydrophobicity of the coating and promotes nanoparticle aggregation during solvent evaporation.[40,41]

The superhydrophobic surface observed in this study was successfully achieved through the synthesis of SiO_2 microbeads and their subsequent modification with hydrophobic silanes. Initially, TEOS underwent hydrolysis and condensation, leading to the formation of SiO_2 microbeads, where the –OH bonds in the untreated paper were replaced with Si–O bonds.[42,43] The introduction of PFOTES and MTES resulted in further hydrolysis and condensation, promoting the development of a nano-micro scale, mountain-like wrinkled structure on the microbeads. This structure, driven by the self-assembly of hydrophobic chains, effectively blocked –OH bonds and hindered water droplets from making contact with the surface. The cross-linking of the acrylic binder between SiO_2 nanoparticles contributes to an additional enhancement of hydrophobicity in the coating.[40] The combination of the rough surface texture, cross-linking of the acrylic binder and the air pockets trapped between the SiO_2 microbeads contributed to the superhydrophobic behaviour, as illustrated in Fig. 2.

Fig. 3 displays the cross-sectional SEM image of the coated paper, which clearly demonstrates that the superhydrophobic coating had penetrated throughout the full thickness of the paper, rather than forming a discrete surface layer. This morphology indicated substantial infiltration of the coating into the substrate, attributed to both the intrinsic absorptive behaviour of the cellulose paper and the specific parameters employed during the coating process. The cellulose paper featured a highly porous microstructure, consisting of an interconnected network of fibres and voids, which readily facilitated the absorption of the coating solution.[44,45] The low viscosity of the superhydrophobic solution further promoted its penetration into the micro- and nano-scale pores within the fibre network. Process conditions, including a prolonged dip time (24 hours aging) and a slow drying rate (1 hour at 80 °C), extended the paper exposure to the coating in its liquid phase, thereby enhancing capillary-driven infiltration.[45,46] This effect was further amplified by the narrow inter-fibre channels that generated strong capillary forces, effectively drawing the coating deep into the paper matrix.[46] As a result, a distinct surface layer was not observed, making it difficult to assess the coating thickness by conventional cross-sectional imaging. To quantitatively estimate the amount of coating deposited, gravimetric analysis was conducted by measuring the weight difference between coated and uncoated samples. Ten samples coated individually (2 cm × 2 cm) were analysed using an analytical balance. The average mass gain was 0.54 mg cm^{-2}, indicating fibre network successfully absorbed the coating and retained synthesized superhydrophobic particles after drying.

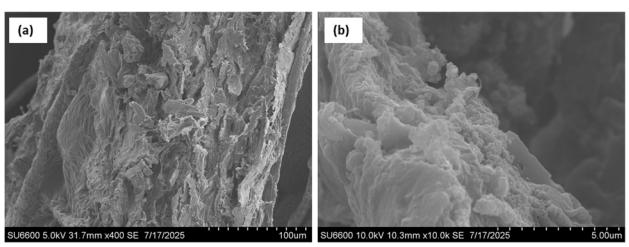

Fig. 3 (a) SEM image of the treated paper surface showing coating material penetrating into the paper matrix, without forming a distinct, continuous coating layer on the surface, and (b) SEM image illustrating the deposition and distribution of coating particles within the fibrous structure of the paper, indicating internal absorption.

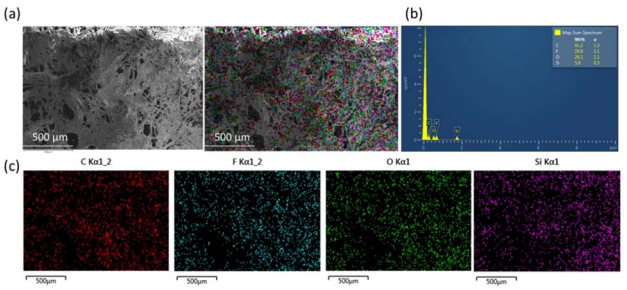

Fig. 4 (a) SEM image utilized for EDX mapping, (b) EDX analysis, and (c) elemental mapping images.

The homogeneous distribution of C, F, O, and Si elements observed in the EDX mapping images (Fig. 4) further confirms the uniform coverage of the treated paper with TEOS, PFOTES, MTES, and the acrylic binder. The widespread presence of F atoms in the analysed area indicates that the surface was thoroughly coated with PFOTES, which offers superior water repellency compared to MTES. In this context, the $-CH_3$ groups derived from MTES contribute to hydrophobicity, while the $-CF_3$ groups introduced by PFOTES significantly enhance hydrophobic performance by further lowering the surface energy.[31,47] The hierarchy of functional groups affecting surface energy reduction is $-CH_2 < -CH_3 < -CF_2 < -CF_2H < -CF_3$.[31,47] Therefore, combining PFOTES with MTES yields superior performance compared to using MTES alone.

The AFM image analysis also shows the hierarchical structure with micro-nano scale roughness. The superhydrophobic coating applied on the smooth non-treated paper has an average surface roughness (Ra) of 124 nm, as determined by AFM (Fig. 5a and b). This indicates that the applied coating created micro clusters and the micro-nano dual structure on the paper, resulting in superhydrophobicity.[12,48]

3.3 Chemical composition

The FTIR spectra of non-treated and treated paper surfaces are illustrated in Fig. 6a and b. The non-treated paper spectrum shows an absorption band at 3332 cm^{-1}, which corresponds to

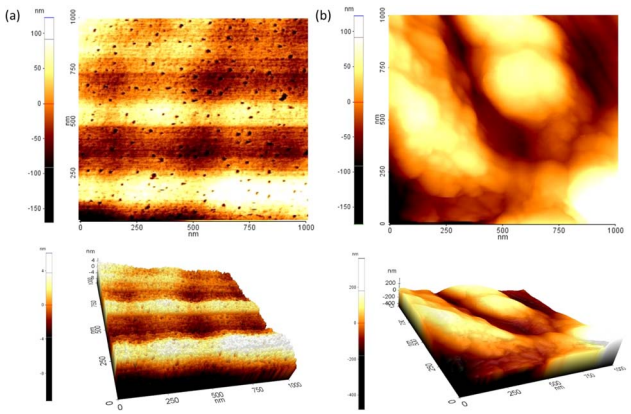

Fig. 5 AFM images of (a) non-treated paper, and (b) treated paper.

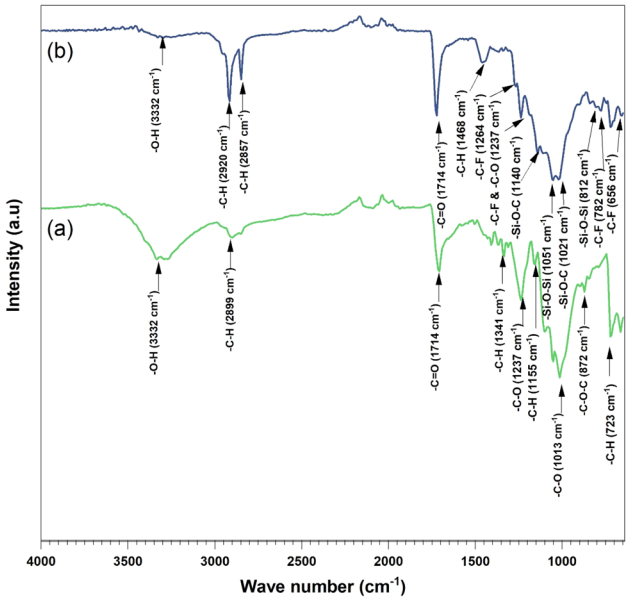

Fig. 6 FTIR spectra of (a) non-treated paper, and (b) treated paper.

the stretching of –OH in cellulose.[49,50] Bands at 2899 cm^{-1} and 1341 cm^{-1} correspond to the stretching and deformation vibrations of the $-CH_2$ groups in the glucose units of paper cellulose.[50] An absorption band at 872 cm^{-1} suggests β-glycosidic connections between glucose units in cellulose.[49] The signals at 1237 cm^{-1} and 1013 cm^{-1} are the –C–O– group of secondary alcohols and ethers in the cellulose chain backbone.[49–51] The sharp band at 1714 cm^{-1} reflects the carbonyl groups added to the cellulose in the oxidative and reductive bleaching processes of the paper.[52]

The presence of SiO_2 from TEOS, MTES, and PFOTES results in asymmetric stretching and bending vibration of Si–O–Si bonds, which causes the absorption bands at 1051 cm^{-1} and 812 cm^{-1} on the treated paper surface.[53] The two absorption bands at 656 cm^{-1}, 1237 cm^{-1}, and 1264 cm^{-1} are caused by –C–F stretching vibrations of the PFOTES molecules' $-CF_3$ and $-CF_2$ groups.[53–57] In comparison to Fig. 6a, the broad band at 3332 cm^{-1} is much less intense in Fig. 6b. This is due to –OH stretching vibrations from the residual hydroxyl groups in the cellulose after superhydrophobic treatment. The C–O–C pyranose ring skeletal vibration is represented by a strong band around 872 cm^{-1}, as seen in Fig. 6a.[58,59] The peaks at 2920 cm^{-1} and 2857 cm^{-1} are associated with the asymmetric and symmetric stretching vibrations of $-CH_2$ groups in MTES, PFOTES, acrylic binder, and cellulose, respectively. The peak at 1468 cm^{-1} corresponds to the $-CH_2$ and $-CH_3$ deformation vibrations of the acrylic binder.[60] The bands mentioned above in non-treated papers remained the same in treated papers as well. Prominent bands at 1021 cm^{-1} and 1140 cm^{-1} indicate Si–O–C bonds, revealing that silane molecules are securely bound to the cellulose in the paper surface.[54,61,62] These findings demonstrate that TEOS, MTES, acrylic binder, and PFOTES molecules can self-assemble on the paper surface, forming a superhydrophobic layer there.

3.4 Wettability

Non-treated papers are readily deformed when in contact with water. After applying the superhydrophobic coating, water droplets immediately roll off from the paper surface due to the potent water-repellent property of the coating. Water droplets have a WCA of 152° ± 2° and a WSA of 7° ± 0.5° with the treated paper surface, forming a mirror-like reflection when immersed in water and remains non-wet after removal. This implies the presence of an air cushion between the treated paper surface and water, due to the developed dual hierarchical roughness on the paper surface to provide outstanding water repellency.[12,15] (Fig. 7)

Here, to evaluate the uniformity of the superhydrophobic coating, static WCA measurements were conducted at ten randomly selected locations on a coated paper sample. The measured WCAs ranged from 150° to 155°, with a standard deviation of 1°, indicating excellent surface uniformity. Reproducibility was assessed by independently fabricating five coated paper samples (2 cm × 2 cm) under identical conditions at room temperature (27 °C). These samples exhibited WCAs within the same range, confirming the high reproducibility of the coating process.

3.5 Self-cleaning and durability

All natural surfaces accumulate dirt over time, and cleaning them can be both time-consuming and detrimental to the environment due to the use of harsh surfactants and chemicals. A promising solution to this issue is the application of superhydrophobic coatings, which allow contaminants to be easily removed from surfaces with minimal effort. To test the self-cleaning capabilities of these coatings, mud and soil particles were applied to modified paper surfaces. A drop of mud and a layer of soil particles were spread across the treated paper, and water droplets were then allowed to roll off the surface. As the water droplets moved across the contaminated superhydrophobic paper, they effectively carried away the mud and soil particles, as shown in Fig. 8a, b, and c.

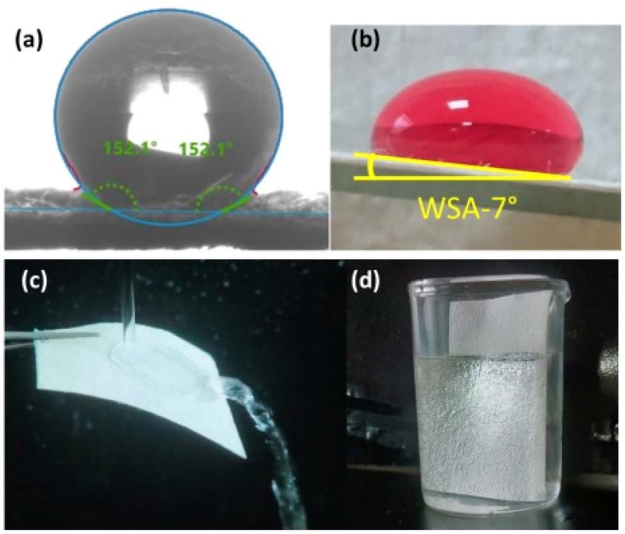

Fig. 7 (a) Water contact angle of treated paper, (b) water sliding angle of the treated paper, (c) water roll off from the treated paper surface, and (d) mirror-like reflection of the paper surface when the treated paper is immersed in water.

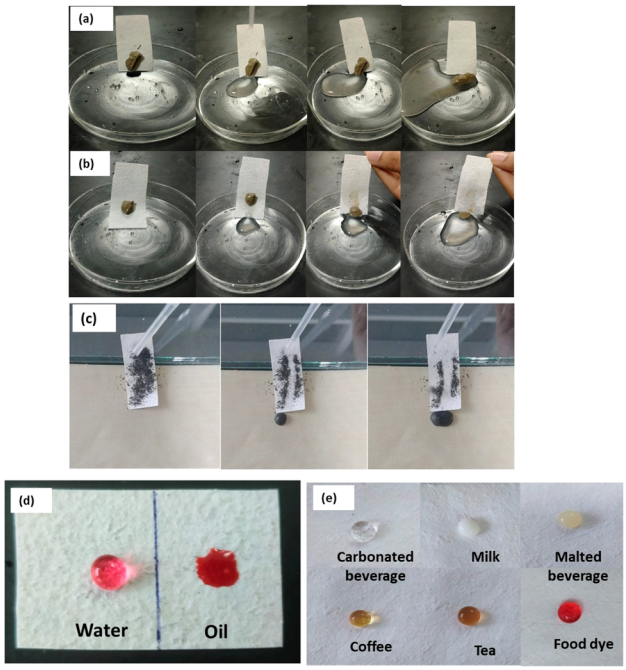

Fig. 8 (a) Self-cleaning test for treated paper with mud, (b) self-cleaning test for non-treated paper with mud, (c) self-cleaning test for treated paper with soil particles, (d) oil absorption of treated paper, and (e) spherical droplet formation by different beverages and dyes on treated paper.

The key to this self-cleaning behavior lies in the micro- and nano-scale roughness of superhydrophobic surfaces. These microscopic structures create a high WCA, causing water droplets to bead up and roll off the surface with ease. As the droplets move, they pick up and carry away contaminants, which have low adhesion to the rough surface. The result is that dirt and debris are efficiently removed without the need for aggressive scrubbing or chemical cleaners. This ability to repel water and contaminants not only makes superhydrophobic surfaces ideal for cleaning but also contributes to reducing the environmental impact of traditional cleaning methods, offering a more sustainable solution to maintaining natural surfaces.[12,63] While superhydrophobic coatings are highly effective at repelling water, they may not exhibit the same level of repellency toward all liquids and contaminants, particularly oils and greases, which are prevalent in the oil and gas construction industry.[64] In many cases, these coatings display oleophilic characteristics, whereby they repel water but simultaneously attract or absorb oils. The superhydrophobic paper surface developed in this study exhibited such selective wettability, demonstrating effective oil absorption alongside water repellency. This combination of properties rendered it a promising candidate for practical applications in oil–water separation (Fig. 8d).

The feasibility of the coating was evaluated using various water-based beverages, including tea, milk, coffee, carbonated

drinks, malted beverages, and food dyes, to assess its liquid-repellent performance. As shown in Fig. 8e, the treated paper surface exhibited typical superhydrophobic behaviour, with all liquid droplets forming nearly perfect spheres and a high WCA of 150°–152° (exceeding the 150° threshold for superhydrophobicity). In addition, the droplets rolled off easily at a low WSA of 8°–9° (below the 10° criterion), demonstrating excellent water repellency and significantly enhancing the surface's potential for practical applications.

The mechanical endurance of the superhydrophobic paper surface was determined using an abrasion test on sandpaper (P-2000 grit). Superhydrophobic paper measuring 2.5 cm × 2.5 cm and weighing 50 g was placed on sandpaper and pushed 10 cm back and forth using the handcrafted abrasion test apparatus. The rotational motion was performed at a rate of 12 cycles per minute. After 50 abrasion cycles, the treated paper retained a WCA of more than 150° and remained entirely dry after immersion in water, showing long-term water repellency (Fig. 9a and b).

Tensile tests were conducted on both treated and untreated paper samples, and the tensile strength of the non-treated paper increased from approximately 2 MPa to approximately 6 MPa after being treated with a superhydrophobic coating (Fig. 9c). The application of superhydrophobic treatment led to a significant increase in the modulus of elasticity (Young's modulus) of untreated paper, rising from 285.02 MPa to 620.94 MPa, thereby enhancing the stiffness and resistance to deformation of the paper. The long-term durability of treated paper was evaluated in chemically hostile circumstances at various pH values. Corrosion from strong acidic or basic liquids can erode the geometrical microstructure of a solid surface, leading to a shift in contact angle.[37] It showed that the wettability of the coating still preserves its superhydrophobicity in the pH range from 5 to 11 (Fig. 9d).

Further, after bending the treated paper 5 times, the crease exhibited strong water resistance (WCA-150°), indicating that the superhydrophobic coating adhered well to the paper surface, as shown in the cross-sectional SEM images (Fig. 3). This observation suggested that the coating maintained its structural integrity and functional properties even under mechanical deformation. The persistence of water repellency along the fold line demonstrated the robustness of the coating-substrate interaction, confirming that the treatment not only forms a uniform hydrophobic layer but also possesses mechanical durability, which is crucial for practical applications where flexibility and handling are required (Fig. 10a and b).

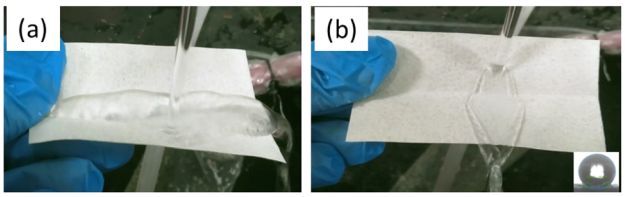

Fig. 10 (a) water flowing along the crease of treated paper after bending 5 times, and (b) the treated paper after exposure to water flow along the bent line.

3.6 Writability and printability

Many superhydrophobic papers reported in the literature fail to accommodate ink adhesion due to excessively low surface energies, resulting in ink beading, smearing, or complete rejection.[65,66] These limitations hinder their applicability in settings where direct user interaction or printed information is essential. The superior performance observed in our study arises not from conventional ink-substrate interaction mechanisms alone, but from a deliberate and optimized design that integrates surface topography and chemistry. This allows the material to function effectively in practical applications that demand both high water repellency and reliable ink adhesion. After treatment with the novel superhydrophobic coating, the paper retained a visual and tactile quality similar to that of untreated cellulose paper, enabling smooth and effective ink deposition using standard writing instruments and printing techniques.

The treated paper retained its superhydrophobic properties after being written on with a pen, pencil, or permanent marker, as illustrated in Fig. 11a–d. The measured WCA for the pristine surface was 152.7° ± 1°, exhibiting only slight reductions after writing: 151.4° ± 1° with the pen, 152.0° ± 1° with the pencil, and 150.5° ± 1° with the permanent marker. These marginal variations in WCA indicated that the water-repellent functionality of the paper remains largely intact despite the application of different writing instruments.

The enhanced writability of this superhydrophobic paper resulted from a carefully engineered combination of surface morphology and chemical composition with a more balanced surface energy compared to traditional superhydrophobic coatings. This allows sufficient water repellency while retaining localized high-energy regions that promote ink anchoring.[67] The hierarchical micro- and nanoscale roughness plays a crucial role in this behavior. These surface textures trap air and maintain

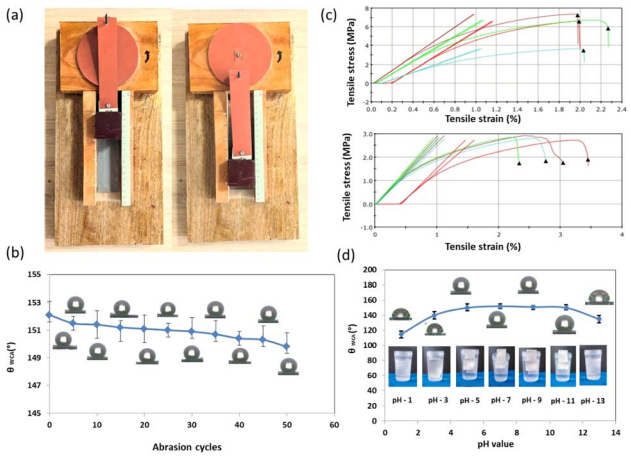

Fig. 9 (a) Abrasion test, (b) graph of WCA under different abrasion cycles, (c) tensile measurements of treated papers (graphs in the above figure) and non-treated papers (graphs in the below figure), and (d) variations in superhydrophobicity of treated paper across different pH levels.

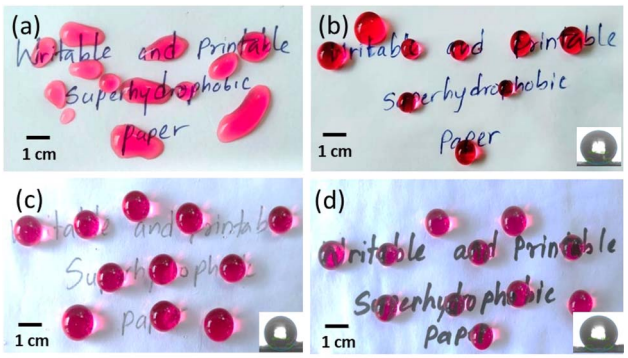

Fig. 11 Comparison of water resistance on written surfaces: (a) non-treated paper written with the pen, (b) treated paper written with the pen, (c) treated paper written with the pencil, and (d) treated paper written with the permanent marker.

water repellency, yet also provide capillary sites where ink can adhere through localized interactions.[15,68] The ink, which contains oil-based solvents and pigments or dyes, partially wets the surface *via* capillary action and spreads within the texture without excessive smearing or runoff. These interactions are further governed by surface energy modulation, which enables the formation of well-defined and stable markings.

During the writing process, the ink solvents contribute to a secondary mechanism that enhances ink fixation. Specifically, the solvents in ink can partially dissolve the superhydrophobic coating, allowing the ink to penetrate toward the underlying paper matrix. As the solvent evaporates, the dissolved coating components re-deposit as a thin, transparent layer, effectively sealing the ink in place. Simultaneously, the ink pigments or dyes become mechanically interlocked within the porous paper structure. This process enhances both the durability and clarity of the written content, while the surface retains its superhydrophobicity.

Remarkably, the paper also retained its superhydrophobic characteristics even after printing with the laser printer, as

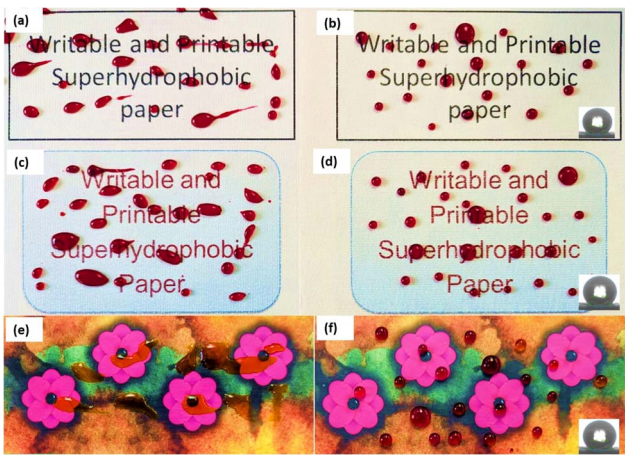

Fig. 12 Comparison of water resistance on printed paper surfaces: (a) untreated paper with black and white printing, (b) treated paper with black and white printing, (c) untreated paper with colour text printing, (d) treated paper with colour text printing, (e) untreated paper with colour figure printing, and (f) treated paper with colour figure printing.

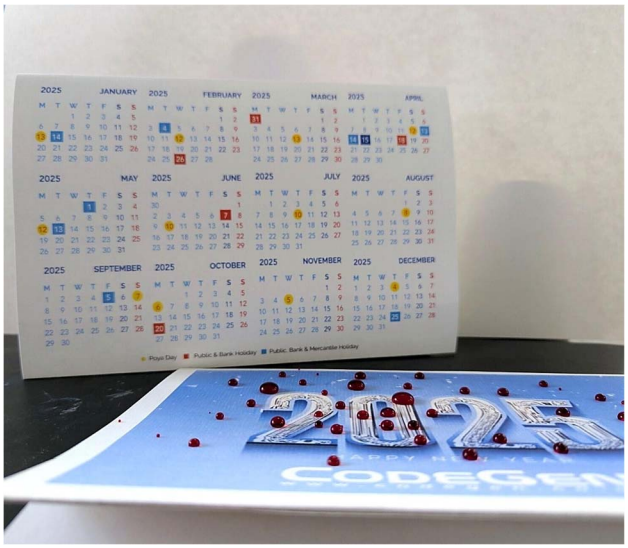

Fig. 13 Superhydrophobic desk calendar.

illustrated in Fig. 12a–f. The measured WCA of 150.2° ± 0.5° on the printed surface confirmed that the laser printing process had minimal impact on the water-repellent performance of the surface, demonstrating the robustness and durability of the superhydrophobic coating. In contrast, inkjet printing proved ineffective, as the water-based ink was unable to adhere to the treated surface due to the high repellency of the superhydrophobic layer.[69,70] This difference is attributed to the contrasting printing mechanisms: inkjet printing relies on ink wetting and binding to the substrate, which is hindered by the low surface energy of superhydrophobic materials, leading to poor adhesion and print failure.[71] In contrast, laser printing uses dry toner fused to the surface through heat and pressure, a process independent of surface wettability. This allows for effective toner adhesion and durable print quality, while preserving the water-repellent properties of the surface.[71,72] As demonstrated, laser printing is thus a more suitable and reliable method for marking superhydrophobic papers.[71,72]

Fig. 13 illustrates the practical application of the superhydrophobic paper as a desk calendar. An ivory board was coated with the superhydrophobic coating and printed using a RICOH Pro C5210S laser printer.

Overall, the findings demonstrated that it is possible to reconcile superhydrophobicity with writability and printability through strategic surface engineering. The resulting material holds promise for multifunctional applications such as water-resistant documents, self-cleaning labels, anti-fouling coatings, and advanced printable substrates for electronics, packaging, or security printing. This represents a significant step forward in expanding the practical utility of superhydrophobic surfaces beyond passive water resistance.

4 Conclusions

This study developed a simple and effective method for creating superhydrophobic paper using the dip coating technique. The

experimental results showed that forming nano/microstructures on the treated paper surface created superhydrophobicity with a WCA of 152° ± 2° and a WSA of 7° ± 0.5°. The deposition of SiO_2 microbeads with nano-micro scale mountain-like wrinkled coating on paper maintained superhydrophobicity even after 50 abrasions on sandpaper and increased the tensile strength from ~2 MPa to ~6 MPa compared to untreated paper. The modified paper exhibited excellent self-cleaning ability and retained superhydrophobicity when exposed to various liquid solutions such as acids & bases (pH 5–11), everyday beverages, and food colors. Importantly, engineered paper has the ability to print and write, and the water repellent properties of the paper are maintained after printing or writing due to the precisely built oleophilic and hydrophobic coating on its surface. This innovative, simple dip coating approach generates superhydrophobicity on the surface of paper, which opens up the possibility of expanding the range of practical applications for paper by designing superhydrophobic books, newspapers, magazines, and paintings.

Author contributions

V. G. C. Samanmali: conceptualization, methodology, writing – original draft, data curation, investigation, visualization, formal analysis. A. R. M. A. M. Rathnayake: writing – review & editing, visualization, formal analysis, data curation, investigation. Nishan Dharmaweera: writing – review & editing, supervision, validation, data curation. M. M. M. G. P. G. Mantilaka: writing – review & editing, supervision, validation, data curation, funding acquisition, resources, investigation. T. Bandara: writing – review & editing, supervision, validation, data curation, investigation. R. T. De Silva: writing – review & editing, supervision, investigation.

Conflicts of interest

There are no conflicts to declare.

Data availability

All data used in this study are presented in the manuscript.

Acknowledgements

This work was supported by CodeGen International (Pvt) Ltd.

Notes and references

1 D. W. Li, *et al.*, Large-scale fabrication of durable and robust super-hydrophobic spray coatings with excellent repairable and anti-corrosion performance, *Chem. Eng. J.*, 2019, **367**, 169–179.
2 E. C. Cho, *et al.*, Robust multifunctional superhydrophobic coatings with enhanced water/oil separation, self-cleaning, anti-corrosion, and anti-biological adhesion, *Chem. Eng. J.*, 2017, **314**, 347–357.
3 A. Romero-Montero, *et al.*, Oil/water separation by superhydrophobic wastepaper cellulose-candelilla wax cryogel: a circular material-based alternative, *Front. Mater.*, 2023, **10**, 1–10, DOI: 10.3389/fmats.2023.1308094.
4 F. Wang, *et al.*, Anti-icing performance of transparent and superhydrophobic surface under wind action, *J. Sol-Gel Sci. Technol.*, 2015, **75**(3), 625–634.
5 L. Sha, *et al.*, Facile fabrication of superhydrophobic filter paper with improved durability and water repellency, *Nord. Pulp Pap. Res. J.*, 2021, **36**(4), 662–670.
6 L. Wang, *et al.*, Anti-fogging performances of liquid metal surface modified by ZnO nano-petals, *J. Taiwan Inst. Chem. Eng.*, 2019, **95**, 65–70.
7 J. Yoon, *et al.*, Wet-Style Superhydrophobic Antifogging Coatings for Optical Sensors, *Adv. Mater.*, 2020, **32**(34), 2002710.
8 K. M. Wisdom, *et al.*, Self-cleaning of superhydrophobic surfaces by self-propelled jumping condensate, *Proc. Natl. Acad. Sci. U. S. A.*, 2013, **110**(20), 7992–7997.
9 H. Ogihara, *et al.*, Simple Method for Preparing Superhydrophobic Paper: Spray- Deposited Hydrophobic Silica Nanoparticle Coatings Exhibit High Water-Repellency and Transparency, *Langmuir*, 2012, **23**, 4605–4608.
10 X. Feng and L. Jiang, Design and creation of superwetting/antiwetting surfaces, *Adv. Mater.*, 2006, **18**(23), 3063–3078.
11 X. Zhang, *et al.*, Superhydrophobic surfaces: From structural control to functional application, *J. Mater. Chem.*, 2008, **18**(6), 621–633.
12 Y. Teng, *et al.*, Facile fabrication of superhydrophobic paper with durability , chemical stability and self - cleaning by roll coating with modified nano - TiO_2, *Appl. Nanosci.*, 2020, **10**, 4063–4073.
13 M. Jin, *et al.*, Review: Natural Superhydrophobic Surfaces and Applications, *J. Biomater. Nanobiotechnol.*, 2020, **11**(02), 110–149.
14 F. Guan, *et al.*, Preparation of hydrophobic transparent paper *via* using polydimethylsiloxane as transparent agent, *J. Bioresour. Bioprod.*, 2020, **5**(1), 37–43.
15 S. Liu, *et al.*, Printable and Versatile Superhydrophobic Paper *via* Scalable Nonsolvent Armor Strategy, *ACS Nano*, 2022, **16**(6), 9442–9451.
16 A. Baidya, *et al.*, Organic Solvent-Free Fabrication of Durable and Multifunctional Superhydrophobic Paper from Waterborne Fluorinated Cellulose Nanofiber Building Blocks, *ACS Nano*, 2017, **11**(11), 11091–11099.
17 B. Qian and Z. Shen, Fabrication of superhydrophobic surfaces by dislocation-selective chemical etching on aluminum, copper, and zinc substrates, *Langmuir*, 2005, **21**(20), 9007–9009.
18 Y. Cheng, *et al.*, A novel strategy for fabricating robust superhydrophobic fabrics by environmentally-friendly enzyme etching, *Chem. Eng. J.*, 2019, **355**, 290–298.
19 A. Pakdel, *et al.*, Plasma-assisted interface engineering of boron nitride nanostructure films, *ACS Nano*, 2014, **8**(10), 10631–10639.
20 D. Wang, *et al.*, Design of robust superhydrophobic surfaces, *Nature*, 2020, **582**(7810), 55–59.

21 Z. Li, *et al.*, Surface-Embedding of Functional Micro-/Nanoparticles for Achieving Versatile Superhydrophobic Interfaces, *Matter*, 2019, **1**(3), 661–673.
22 C. Peng, *et al.*, All-organic superhydrophobic coatings with mechanochemical robustness and liquid impalement resistance, *Nat. Mater.*, 2018, **17**(4), 355–360.
23 A. Stamm, Brief-Thermal Degradation of Wood and Celluiose, *Ind. Eng. Chem.*, 1956, **48**(3), 413–417.
24 H. Yang and Y. Deng, Preparation and physical properties of superhydrophobic papers, *J. Colloid Interface Sci.*, 2008, **325**(2), 588–593.
25 H. Lei, *et al.*, Fluorine-free superhydrophobic coatings based on silicone and functionalized colloidal silica, *Coatings*, 2019, **9**(3), 159.
26 Q. Wang, *et al.*, Fluorine-free superhydrophobic coatings from polydimethylsiloxane for sustainable chemical engineering: Preparation methods and applications, *Chem. Eng. J.*, 2021, **426**(8), 130829.
27 Y. C. Sheen, *et al.*, Non-fluorinated superamphiphobic surfaces through sol-gel processing of methyltriethoxysilane and tetraethoxysilane, *Mater. Chem. Phys.*, 2009, **114**(1), 63–68.
28 T. Sepperer, *et al.*, Fluorine free surface modification of tannin-furanic foams by silylation, *Mater. Des.*, 2023, **230**, 111936.
29 X. Gong and S. He, Highly Durable Superhydrophobic Polydimethylsiloxane/Silica Nanocomposite Surfaces with Good Self-Cleaning Ability, *ACS Omega*, 2020, **5**(8), 4100–4108.
30 K. Aminuddin, *et al.*, Fluorine-free Superhydrophobic Stearic Acid Modified Kaolin Nanoparticles for Self-cleaning Silicone Rubber Surface, *J. Fundam. Appl. Sci.*, 2024, **20**(3), 661–668.
31 Q. Li, *et al.*, Super-hydrophobic Hybrid Coatings Preparation used by Methyltrithoxysilane (MTES) and Tetraethylorthosilicate(TEOS), *7 th International Conference on the Durability of Concrete Structures*, 2022.
32 J. Saengkaew, *et al.*, Superhydrophobic coating from fluoroalkylsilane modified natural rubber encapsulated SiO 2 composites for self-driven oil/water separation, *Appl. Surf. Sci.*, 2018, **462**, 164–174.
33 C. Malins, *et al.*, Influence of the surface polarity of dye-doped sol-gel glass films on optical ammonia sensor response, *Thin Solid Films*, 2000, **368**(1), 105–110.
34 M. G. Shange, *et al.*, Factors Affecting Silica/Cellulose Nanocomposite Prepared *via* the Sol–Gel Technique: A Review, *Materials*, 2024, **17**(9), 1–23.
35 K. Dlomo, *et al.*, Influence of silica nanoparticles on the properties of cellulose composite membranes: A current review, *Cellul. Chem. Technol.*, 2020, **54**(7–8), 765–775.
36 J. Estella, *et al.*, Effects of aging and drying conditions on the structural and textural properties of silica gels, *Microporous Mesoporous Mater.*, 2007, **102**(1–3), 274–282.
37 M. Zhang, *et al.*, Fabrication of coral-like superhydrophobic coating on filter paper for water-oil separation, *Appl. Surf. Sci.*, 2012, **261**, 764–769.
38 X. Jiang, *et al.*, Preparation and Characterization of Degradable Cellulose-Based Paper with Superhydrophobic, Antibacterial, and Barrier Properties for Food Packaging, *Int. J. Mol. Sci.*, 2022, **23**(19), 13.
39 M. He, *et al.*, Controllable stearic acid crystal induced high hydrophobicity on cellulose film surface, *ACS Appl. Mater. Interfaces*, 2013, **5**(3), 585–591.
40 V. V. Klimov, *et al.*, Formation of Superhydrophobic Coatings Based on Dispersion Compositions of Hexyl Methacrylate Copolymers with Glycidyl Methacrylate and Silica Nanoparticles, *Polymers*, 2024, **16**(21), 3094.
41 E. V. Bryuzgin, *et al.*, Aluminum surface modification with fluoroalkyl methacrylate-based copolymers to attain superhydrophobic properties, *Appl. Surf. Sci.*, 2017, **419**, 454.
42 G. De, *et al.*, Hydrolysis-condensation reactions of TEOS in the presence of acetic acid leading to the generation of glass-like silica microspheres in solution at room temperature, *J. Mater. Chem.*, 2000, **10**(10), 2289–2293.
43 M. C. B. Salon and M. N. Belgacem, Competition between hydrolysis and condensation reactions of trialkoxysilanes, as a function of the amount of water and the nature of the organic group, *Colloids Surf., A*, 2010, **366**(1–3), 147–154.
44 D. W. Wei, *et al.*, Superhydrophobic modification of cellulose and cotton textiles: Methodologies and applications, *J. Bioresour. Bioprod.*, 2020, **5**(1), 1–15.
45 H. Teisala, *et al.*, Superhydrophobic Coatings on Cellulose-Based Materials: Fabrication, Properties, and Applications, *Adv. Mater. Interfaces*, 2014, **1**(1), 1300026.
46 K. Manoharan, *et al.*, Development of hydrophobic paper substrates using silane and sol–gel based processes and deriving the best coating technique using machine learning strategies, *Sci. Rep.*, 2021, **11**(1), 11352.
47 S. Yang, *et al.*, Low-surface-energy fluoromethacrylate block copolymers with patternable elements, *Chem. Mater.*, 2000, **12**(1), 33–40.
48 X. Zeng, *et al.*, Polymer-infiltrated approach to produce robust and easy repairable superhydrophobic mesh for high-efficiency oil/water separation, *J. Mater. Sci.*, 2018, **53**(14), 10554–10568.
49 B. Abderrahim, *et al.*, Kinetic Thermal Degradation of Cellulose, Polybutylene Succinate and a Green Composite: Comparative Study, *World J. Environ. Eng.*, 2015, **3**(4), 95–110.
50 Z. Luo, *et al.*, A glucose modified filter paper for effective oil/water separation, *RSC Adv.*, 2018, **8**(52), 29570–29577.
51 D. Shao and Q. Wei, Microwave-assisted rapid preparation of nano-ZnO/Ag composite functionalized polyester nonwoven membrane for improving its UV shielding and antibacterial properties, *Materials*, 2018, **11**(8), 1412.
52 U. Henniges and A. Potthast, Bleaching revisited: Impact of oxidative and reductive bleaching treatments on cellulose and paper, *Restaurator*, 2009, **30**(4), 294–320.
53 C. Liu, F. Su and J. Liang, Facile fabrication of a robust and corrosion resistant superhydrophobic aluminum alloy surface by a novel method, *RSC Adv.*, 2014, **4**(98), 55556–55564.
54 J. D. Brassard, *et al.*, Fluorine based superhydrophobic coatings, *Appl. Sci.*, 2012, **2**(2), 453–464.

55 K. Teshima, *et al.*, Gas barrier performance of surface-modified silica films with grafted organosilane molecules, *Langmuir*, 2003, **19**(20), 8331–8334.
56 D. L. Setyaningrum, *et al.*, Analysis of corn and soybean oils in red fruit oil using FTIR spectroscopy in combination with partial least square, *Int. Food Res. J.*, 2013, **20**(4), 1977–1981.
57 R. qing Liu, *et al.*, New collectors for the flotation of unactivated marmatite, *Miner. Eng.*, 2010, **23**(2), 99–103.
58 A. Haider, *et al.*, A novel use of cellulose based filter paper containing silver nanoparticles for its potential application as wound dressing agent, *Int. J. Biol. Macromol.*, 2018, **108**, 455–461.
59 J. Li, *et al.*, Microwave-assisted solvent-free acetylation of cellulose with acetic anhydride in the presence of iodine as a catalyst, *Molecules*, 2009, **14**(9), 3551–3566.
60 Q. Yong and C. Liang, Synthesis of an aqueous self-matting acrylic resin with low gloss and high transparency *via* controlling surface morphology, *Polymers*, 2019, **11**(2), 322.
61 A. S. Zakirov, *et al.*, Comparative study on the structural and electrical properties of low-k SiOC(-H) films deposited by using plasma enhanced chemical vapor deposition, *J. Korean Phys. Soc.*, 2007, **50**(6), 1809–1813.
62 A. Paryab, *et al.*, Manufacturing and structural evaluation of polymer derived sioc/tic and SiOC/TiC/mullite nanocomposites, *Iran. J. Mater. Sci. Eng.*, 2021, **18**(3), 1–8.
63 R. Fürstner, *et al.*, Wetting and self-cleaning properties of artificial superhydrophobic surfaces, *Langmuir*, 2005, **21**(3), 956–961.
64 A. Waqar, *et al.*, Evaluation of Success of Superhydrophobic Coatings in the Oil and Gas Construction Industry Using Structural Equation Modeling, *Coatings*, 2023, **13**(3), 526.
65 M. Elsharkawy, *et al.*, Inkjet patterned superhydrophobic paper for open-air surface microfluidic devices, *Lab Chip*, 2014, **14**(6), 1168–1175.
66 N. Singh and A. Ghatak, Hierarchically Rough Surface Used as Rewritable and Reprintable Paper, *arXiv*, 2021, preprint, arXiv:2111.12430, DOI: **10.48550/arXiv.2111.12430**.
67 Y. Liu, *et al.*, Enhancing ink adhesion of specialty paper using an interpenetrating polyvinyl alcohol-blocked polyurethane polymer network sizing system, *RSC Adv.*, 2022, **12**(21), 13267–13278.
68 Y. Tang, *et al.*, Advancements in Superhydrophobic Paper-Based Materials: A Comprehensive Review of Modification Methods and Applications, *Nanomaterials*, 2025, **15**(2), 107.
69 M. J. Docherty, *et al.*, Inkjet Printing on Hydrophobic Surface: Practical Implementation of Stacked Coin Strategy, *Adv. Eng. Mater.*, 2024, **26**(11), 2400237.
70 T. J. Dannhauser, D. E. Bugner, D. D. Putnam and B. L. Lindstrom, *US Pat.*, 9376582B1, 2016.
71 D. Barona and A. Amirfazli, Producing a superhydrophobic paper and altering its repellency through ink-jet printing, *R. Soc. Chem.*, 2011, **11**(5), 936–940.
72 C. V. Ngo and D. M. Chun, Laser Printing of Superhydrophobic Patterns from Mixtures of Hydrophobic Silica Nanoparticles and Toner Powder, *Sci. Rep.*, 2016, **6**, 36735.